Dynamics of Low Molecular Weight DNA Fragments in Dilute and Semidilute Solutions

Hidde Tj. Goïnga† and R. Pecora*

Department of Chemistry, Stanford University, Stanford, California 94305-5080

Received December 27, 1990; Revised Manuscript Received July 6, 1991

ABSTRACT: The scattered light intensity autocorrelation functions of dilute and semidilute solutions of sonicated calf thymus DNA fragments in the presence of 0.2 M NaCl were measured. In addition, the weight-average molecular weight and the second virial coefficient of this system were determined by low-angle laser light scattering (LALLS). The weight-average molecular weight was found to be (1.56 ± 0.05) × 10^5, corresponding to a fragment size of 236 ± 8 base pairs, and the second virial coefficient was (2.7 ± 0.2) × 10^{-7} (mol L g^{-2}). The scattered light intensity correlation functions were analyzed by three different methods of data analysis: CONTIN, the method of cumulants, and a double-exponential fitting procedure. CONTIN gave evidence of the existence of a single relaxation process at low DNA concentrations and an additional slower process at DNA concentrations higher than ~2 g L^{-1}. The rates of the fast and slow processes were shown to vary linearly with the square of the length of the scattering vector q. The fast mode was interpreted as the translational diffusion process of the DNA fragments. The measured mutual diffusion coefficient was found to increase linearly with the DNA concentration. The infinitely dilute solution value of the mutual diffusion coefficient was determined by extrapolation and is in excellent agreement with the theoretical value for a perfectly rigid rod, calculated according to the Tirado and Garcia de la Torre theory. The second virial coefficient is in reasonable agreement with theory if charge effects, as proposed by Stigter, are taken into account. The molecular origin of the slow mode is still unknown, although its behavior is consistent with the formation of aggregates at high DNA concentrations. The aggregates are probably highly polydisperse. The amplitude and diffusion coefficient of the slow process appeared to decrease with increasing DNA concentration. The results are in poor agreement with the predictions of the Doi, Shimada, and Okano theory for semidilute and concentrated solutions of hard, rigid rods as well as that for such systems near the spinodal.

Introduction

Much interest has recently been focused on the dynamics of rodlike macromolecules in both dilute and nondilute solutions. These macromolecules are of great importance in both biology and materials science and, in addition, provide a fertile area of application for fundamental statistical mechanics.

A large body of experimental and theoretical work has followed the pioneering theoretical work of Doi and Edwards (DE). The DE theory in its simplest form is a scaling theory of the dynamics of uncharged rodlike molecules in nondilute solutions based on the reptation concept used for flexible polymers.[1,2] DE define several concentration regimes depending on the average distance between the rods in solution. The average distance between rods of length L and diameter d in a solution with C rods per unit volume is $1/C^{1/3}$. In the *dilute* regime the average distance between rods is much larger than the length of the rod ($C \ll 1/L^3$): the rods can rotate and translate freely without hindrance by other polymers. As the concentration increases, the diffusion of the rods becomes restricted as a result of the hard-core repulsion between the rods. At concentrations well above $1/dL^2$ the rods order and form liquid crystal phases. The solution is no longer isotropic. The *semidilute* region is defined as the concentration region much larger than $1/L^3$ but smaller than $1/dL^2$. In this regime rotational and translational diffusion are restricted but the solution is still isotropic.

According to the assumptions of the DE theory, in semidilute solutions translation of rods perpendicular to the rod's main axis is prohibited. Translation parallel to the main axis of the rod is still unrestricted by the other rods. Thus, in the DE theory the translational diffusion coefficient of rods in semidilute solution reduces to half its value in infinitely dilute solutions and, at least in the semidilute region, is concentration independent. It should be emphasized that the DE theory assumes the rods to be perfectly rigid and infinitely thin. No intermolecular interactions other than that the rods cannot pass through each other are taken into account in this version of the DE theory. The solutions are thermodynamically ideal.

Subsequent theoretical work and Brownian dynamics work by Fixman[3] have presented an alternative point of view to the reptation theories (often called "caging theories" in the case of rigid rods) based on cooperative motions of the rods. Fixman's theory focuses mainly on the rotational relaxation. Brownian dynamics simulations by Bitsanis et al.,[4] which include simulations of both rotational and translational diffusion, indicate that the Fixman theory appears to agree with the simulations at the lower CL^3 in the semidilute region and that the Doi–Edwards based caging theories take over at much higher concentrations. These theories generally treat the motion of a single rod and do not compute the dynamic structure factor that is measured in polarized dynamic light scattering (DLS) experiments.[5] A mean-field theory of the dynamic structure factor for hard-rod systems has been presented by Doi, Shimada, and Okano (DSO-I).[6] DSO-I assumes the usual coupled rotation–translation diffusion equation for the single-rod motion and then computes the DLS structure factor in the limit of low scattering vector length, recovering the usual result of the phenomenological theory, except that the friction factor in the formula for the mutual diffusion coefficient is the friction factor for self-diffusion rather than that for mutual diffusion and sedimentation. Effects at higher scattering vector lengths which give a wave vector dependent apparent diffusion coefficient are calculated as the next correction term. In DSO-I, the rotational and self-diffusion coefficients are treated as parameters, usually invoking DE assumptions for their values in semidilute solution. A numerical implementation

† Present address: Groensvoorde 154, 2742 DP Waddinxveen, The Netherlands.

0024-9297/91/2224-6128$02.50/0

of this theory has been given by Maeda.[7] DSO also gives a theory of the dynamic structure factor for solutions near the critical concentration at which the isotropic phase becomes unstable (DSO-II).[8] If the concentration of a solution is suddenly brought above the critical concentration, an anisotropic phase separates from the isotropic phase. DSO-II assumes that this phase separation occurs by spinodal decomposition.

A wide range of experimental work done on a variety of rodlike polymers has yet to provide definitive answers to the basic mechanism of translational and rotational motion in semidilute solutions of rods.[9-23] It is clear that for most systems studied the solutions are far from ideal (nonzero thermodynamic second virial coefficient). Most studies of the translational motions of rodlike polymers are conducted using DLS which measures the dynamic structure factor whose decay for short rods usually gives the mutual diffusion coefficient rather than the self-diffusion coefficients treated in DE. The DSO theories,[6,8] as mentioned above, treat the dynamic structure factor for a system of hard rods.

In addition, for various rodlike as well as flexible polyelectrolytes it has been observed that, at high polymer concentrations and at low ionic strengths, the experimental light scattering intensity autocorrelation function shows an additional slow decay ("slow mode").[11-21] (Some authors have also noted the presence of one or more "fast modes" in solutions of short rods, which are often attributed to translational–rotational coupling effects.[10,22-24]) The appearance of the slow decay at low ionic strength has been associated with the transition from an ordinary to an extraordinary phase.[17] It has been suggested that the presence of loose aggregates is responsible for the observed slow decay.[14,25] Fried and Bloomfield[26] attributed the slow mode to the presence of a gellike phase in semidilute solutions of 200 base-pair (bp) DNA fragments.

DNA fragments can be prepared in a wide range of molecular weights. In fact, oligonucleotides (less than about 100 bp) and restriction fragments can be prepared in essentially monodisperse form.[27] The longer restriction fragments deviate from rigid-rod behavior and may be used to investigate the effects of limited flexibility on macromolecular dynamics, while very large molecular weight DNAs are globular. Thus, the entire range of macromolecular conformation may be studied with a single homologous series. Restriction fragments are especially suitable for the study of rodlike molecules in dilute solutions. However, it is often not practically feasible to obtain DNA restriction fragments in quantities large enough to study their behavior in concentrated solutions. For these studies, DNA fragments with relatively narrow, but not monodisperse, molecular weight distributions are normally used.

Wang, Garner, and Yu[12] studied the dynamics of nucleosome DNA with an approximate length of 50 nm (150 bp) in concentrated solutions. Using forced Rayleigh scattering, they observed a decreasing self-diffusion coefficient with concentration, while, at high ionic strengths, the mutual diffusion coefficient (measured by DLS) was reported to remain constant. These results also indicate that the slow component measured in DLS is not the same as the self-diffusion coefficient and that the DE assumption of the reduction of the self-diffusion coefficient to half of its infinite dilution value and its subsequent concentration independence in the semidilute region does not apply in this system.

The same system as in the Wang et al. work was studied by Nicolai and Mandel.[13,14] They measured the dynamic as well as the total intensity light scattering of 150 bp sonicated nucleosome DNA at several ionic strengths and DNA concentrations. At each salt concentration the mutual diffusion coefficient was found to increase linearly with concentration. The values for the coefficient of the linear term in the expansion of the mutual diffusion coefficient in concentration were shown to be consistent with those from theory. The experimental translational diffusion coefficient at infinite dilution was in agreement with that calculated assuming a perfectly rigid rod.

Here we report the results of a study of the concentration effects on the dynamics of short DNA fragments in concentrated solutions in the presence of excess low molecular weight salt. Polyelectrolytes in excess salt solutions behave very similarly to uncharged polymers.[28] The DNA fragments were obtained by extensive sonication of high molecular weight calf thymus DNA and were reported to have a size of 200 ± 30 bp.[26] The infinitely dilute solution values of the translational diffusion coefficient of DNA fragments up to 150 bp have been shown to still obey the theoretical expressions for perfectly rigid rods.[12-14] DNA restriction fragments consisting of more than 367 bp have been shown to significantly depart from perfectly rigid-rod behavior, and some flexibility in the chain has to be taken into account.[29]

DLS of solutions with DNA concentrations up to about 20 g L^{-1} ($CL^3 \simeq 35$) is measured. The DLS intensity autocorrelation functions are analyzed using the method of cumulants, the constrained inverse Laplace transform program, CONTIN, and fits of the data to a sum of two exponentials. The weight-average molecular weight and the second virial coefficient are determined by low-angle laser light scattering (LALLS). The experimental results are compared with those calculated from the phenomenological and DSO theories and with those of previous workers on both the shorter sonicated fragments[12-14] and the longer more globular DNAs.[29-31]

Theory

In the DLS experiments the normalized intensity time autocorrelation function $g_2(\tau)$ was determined. Assuming a Gaussian distribution of the scattered electric field, $g_2(\tau)$ can be related to the normalized electric field autocorrelation function $g_1(\tau)$ by the Siegert relation[5]

$$g_1(\tau) = [g_2(\tau) - 1]^{1/2} \tag{1}$$

For a monodisperse solution of polymers the classical diffusion theory gives[5]

$$g_1(\tau) \propto \exp(-q^2 D_m \tau) \tag{2a}$$

Here D_m is the mutual translation diffusion coefficient and q the length of the scattering vector, which is given by

$$q = (4\pi n/\lambda_0) \sin(\theta/2) \tag{2b}$$

where n is the refractive index of the solvent, λ_0 is the wavelength of the incident light in vacuo, and θ is the observation angle of the scattered light relative to the transmitted beam. For long rodlike polymers extra terms dependent on the rod rotational motion appear in eq 2a. It can be shown,[5] however, that, for rods with lengths smaller than about 100 nm and within the q-range normally accessible in scattering experiments using visible light, the direct contribution of these rotational diffusion terms to the measured correlation function is negligible. For polydisperse systems the normalized electric field autocorrelation function $g_1(\tau)$ is assumed to consist of a sum

of exponentials

$$g_1(\tau) = \int_0^\infty G(\Gamma) \exp(-\Gamma\tau)\, d\Gamma \quad (3)$$

where $G(\Gamma)$ is the distribution function of the frequency $\Gamma \equiv q^2 D_m$.

The phenomenological theory expresses the mutual diffusion coefficient in terms of frictional and thermodynamic parameters[5]

$$D_m = (M/N_{av}f(c))(1 - v_s c)(\partial\Pi/\partial c)_T \quad (4)$$

where M is the polymer molecular weight, N_{av} is Avogadro's number, c is the polymer weight concentration, and v_s is the polymer specific volume. The function $f(c)$ is the concentration-dependent molecular friction coefficient, and $(\partial\Pi/\partial c)_T$ is the concentration derivative of the osmotic pressure. This latter quantity is proportional to the thermodynamic driving force which acts to relax concentration fluctuations.

The friction coefficient may be expanded in a power series in the concentration[5,14]

$$f(c) = f_0(1 + k_f c + ...) \quad (5)$$

where f_0 is the friction coefficient at infinite dilution and $(1 + k_f c)$ represents the change in friction with concentration due to direct physical hindrance and/or hydrodynamic interaction. This friction coefficient is identical to that measured in sedimentation experiments, but, in general, is not the same as that for self-diffusion. (Discussions of this for liquid dispersions of interacting spheres are given by Pusey and Tough[32] and by Schmitz.[33]) After expanding the osmotic pressure in a virial series and combining the result with eqs 4 and 5, the usual expression for D_m to order c is obtained

$$D_m = D_0(1 + k_D c + ...) \quad (6a)$$

with $D_0 \equiv kT/f_0$ and

$$k_D = (2MA_2 - v_s - k_f) \quad (6b)$$

where D_0 is the mutual translational diffusion coefficient at zero concentration, kT has the usual meaning, and A_2 is the osmotic second virial coefficient. D_0 and k_D are determined from the concentration dependence of D_m, which is measured in dynamic light scattering experiments. The molecular weight M and the second virial coefficient A_2 can be determined in static light scattering experiments, and k_f, in principle, from sedimentation experiments. In the Maeda[7] implementation of the DSO theory[6] both A_2 and k_f obtained from DLS experiments are dependent on qL.

Broersma[34] and Tirado and Garcia de la Torre[35] have derived theoretical expressions for the translational diffusion coefficient at infinite dilution (D_0) of cylinders with length L and diameter d:

$$D_0 = (kT/3\pi\eta_s L)[\ln(p) + 0.5(\gamma_{par} + \gamma_{perp})] \quad (7)$$

Here $p = L/d$, η_s is the solvent viscosity, and γ_{par} and γ_{perp} are end effect corrections. The results of the derivations by Broersma and Tirado and Garcia de la Torre differ in the values for γ_{par} and γ_{perp}. According to Broersma

$$\gamma_{par} = -0.58 + 7.4(1/\ln(2p) - 0.34)^2 \quad (8a)$$

$$\gamma_{perp} = 0.50 + 4.2(1/\ln(2p) - 0.39)^2 \quad (8b)$$

These equations are estimated by Broersma to be valid for $9 < L/d < 400$. Tirado and Garcia de la Torre report the following for rods with $2 < L/d < 30$:

$$\gamma_{par} = -0.207 + 0.980/p - 0.133/p^2 \quad (9a)$$

$$\gamma_{perp} = 0.839 + 0.185/p + 0.233/p^2 \quad (9b)$$

To account for possible flexibility in the rod, the polymer may be modeled as a semistiff wormlike chain. Theoretical expressions for the translational diffusion coefficients of wormlike chains have been given by Yamakawa and Fujii.[36] They used a wormlike cylindrical model without excluded volume. The translational diffusion coefficient of a wormlike polymer can be calculated from the Yamakawa and Fujii expressions using the contour length L, the diameter d, and the persistence length P of the molecule.

Theoretical expressions for the second virial coefficient A_2 for a system of *uncharged* rigid rods with diameter d and length L have been given by Zimm, Onsager, and Ishihara.[37-40] The most convenient of these, that of Ishihara, may be written in the form

$$A_2 = (\pi N_{av} d^2 L/M^2) f \quad (10a)$$

where f is given by (with $p = L/d$)

$$f = (1/4)p[1 + (3 + \pi)/(2p) + (\pi/4)/p^2] \quad (10b)$$

Peterson[41] evaluated the sedimentation velocity of uncharged rigid rods in a solution of finite concentration. The rods were modeled as rigid pearl chains, following Kirkwood and Riseman.[42] From Peterson's results for the sedimentation velocity, an estimate of the linear coefficient k_f can be derived

$$k_f = (RT/3\eta_s)(L^2/D_0 M)(3d/8L)^{2/3} \quad (11)$$

where R is the universal gas constant. In principle, k_D can be calculated from theory, using the given expressions for D_0, k_f, A_2, and k_D. Major input parameters for this calculation are the length L, the molecular weight M, the diameter d, and the specific volume v_s of the polymer.

Materials and Methods

Sample Preparation. Calf thymus DNA (Sigma, Type I) was dissolved in 10^{-2} M Tris-HCl (pH 8.0 at 20 °C), 2×10^{-3} M EDTA and 1.1 M NaCl to a final concentration of 1 g/L. After bubbling through nitrogen gas, samples were sonicated for 1 h at ice bath temperature in 1-min intervals using a Model 4710 high-intensity ultrasonic processor (Cole-Parmer Instruments Co.) operating at 25 W and 20 kHz.

Following sonication, the DNA was size fractionated by differential precipitation with poly(ethylene glycol) (PEG) as described elsewhere.[43] The high molecular weight fraction was precipitated with 6% PEG. PEG was added to the supernatant to a final concentration of 12%. The low molar mass DNA in the supernatant precipitated and was dissolved in 10^{-2} M Tris-HCl (pH 8.0 at 20 °C) and 10^{-4} M EDTA (TE buffer). The DNA was subsequently precipitated with ethanol and dissolved in TE buffer containing 0.2 M NaCl (TES buffer).

To determine the approximate molecular weight of the isolated fraction, agarose gel electrophoresis was performed. The DNA molecules in the fraction had an average fragment size of 150–250 bp, consistent with previous reports.[26]

Dilutions were made in TES buffer. Concentrations were determined spectrophotometrically at 260 nm. Solutions were stored at 4 °C.

Dynamic Light Scattering Experiments. The dynamic light scattering apparatus used in these experiments utilized a Spectra Physics Model 165 argon ion laser operating at 488 nm. The laser power used was between 10 and 800 mW. The autocorrelation function of the intensity was measured using a Brookhaven BI2030AT digital correlator with 142 real datapoints,

6 of which were delay channels used to measure the base line. The scattering angles used ranged from 20 to 110°. Prior to measurement the solutions were filtered through a Millex GS 0.22-μm pore size filter (Millipore) into a clean Spectrocell 10-mm square glass cuvette. The samples were centrifuged for 1 h at 5000 rpm to remove air bubbles. The solutions were examined for dust through a 5× microscope while illuminated with laser light. When clean, the solutions were allowed to equilibrate for at least 8 h at 20 °C before measurements were taken. All measurements were done at 20 °C. The data sets were electronically transferred from the Brookhaven correlator to a VAXstation 3200 computer for further analysis. The first datapoint from each data set was not used in the analysis.

Static Low-Angle Laser Light Scattering Experiments. LALLS experiments were performed on a Chromatix KMX-6 apparatus operating at 632.8 nm and at 20 °C temperature. The laser light was vertically polarized. Excess scattering intensities were measured at an average angle of 5° using a 0.15-mm pinhole. The DNA solutions had concentrations in the same range as in the dynamic light scattering experiments. The solutions were allowed to equilibrate at 20 °C for at least 8 h prior to measurements. The solutions were filtered through a 0.22-μm pore size Millex GS filter. We found that if 0.45-μm pore size filters were used, the measured scattering intensity showed much larger fluctuations. Measurements were taken immediately after filtration. During the measurements, the sample was slowly flowed through the cell. Output was recorded on a chart recorded and subsequently analyzed.

Data Analysis

Dynamic Light Scattering Experiments. The measured autocorrelation function $Y(\tau)$, divided by the base line B, represents the normalized intensity autocorrelation function $g_2(\tau)$. Via the Siegert relation (eq 1) the experimental autocorrelation function can be related to the normalized electric field autocorrelation function $g_1(\tau)$:

$$g_1(\tau) = [Y(\tau)/B - 1]^{1/2} \quad (12)$$

The value of the calculated base line was used to normalize the experimental data.

It was assumed that $g_1(\tau)$ has the form given in eq 3. $G(\Gamma)$ can be obtained by solving the inverse Laplace transform (ILT) of the measured autocorrelation function. This constitutes an ill-posed problem in that there is an unbounded number of solutions which fit the data equally well within the precision of the data. Various methods have been developed to extract information on $G(\Gamma)$ from experimentally determined autocorrelation functions.[44-47] In this study the measured correlation functions were analyzed by three different methods.

First, all experimental data were analyzed using the method of cumulants.[45] Data were fit to an expansion up to the second cumulant. The first cumulant K_1 represents the weighted average of the frequency Γ. The second cumulant K_2, suitably normalized by $(K_1)^2$, is a measure of the relative width of the distribution of frequencies.

Second, the experimental field autocorrelation functions $g_1(\tau)$ were analyzed using version 2 of the Fortran program CONTIN. This program and its capabilities are described elsewhere.[30,46,47] Using a constrained regularization method, CONTIN calculates the ILT of the measured correlation function numercially within a given frequency window. CONTIN does not require the number of exponentials (or peaks in the distribution of frequencies $G(\Gamma)$) to be input in advance. The smoothest solution which is still consistent with the data is selected as the final solution. Consequently, CONTIN generally will not overestimate the number of relaxation processes occurring in the system. The input boundaries of the frequency window should be chosen such that all peaks of the final solution are contained within the given frequency window. With this restriction the boundaries do not significantly influence the final solution given by CONTIN.

In the cases where CONTIN gave evidence of two relaxation processes (i.e., two peaks in the frequency distribution), data were also fit to a sum of two exponentials

$$Y(\tau) = B[1 + \{A_1 \exp(-\Gamma_1\tau) + A_2 \exp(-\Gamma_2\tau) + Q\}^2] \quad (13)$$

where A_1, A_2, Γ_1, and Γ_2 are the amplitudes and frequencies of the first and second exponentials, respectively, and Q is a constant accounting for "dust". The Fortran program DISCRETE, which was also written by Provencher, was used for this analysis. DISCRETE can fit data to a discrete sum of exponentials and was set to fitting to a sum of maximally two exponentials in this case.

Static Low-Angle Laser Light Scattering Experiments. The Rayleigh ratio (ΔR_θ) was calculated using the experimentally determined excess scattering intensity of the sample over the solvent (TES-buffer) as shown below

$$\Delta R_\theta = F[(I_\theta/I_0)_{\text{sample}} - (I_\theta/I_0)_{\text{TES-buffer}}] \quad (14)$$

where F is an instrumental constant and I_θ the average intensity of the light scattered at an average angle θ by the TES buffer or the DNA solution which is illuminated with laser light with an intensity I_0. At the small angles used in this experiment ($\theta \sim 5°$), the influence of intra- or intermolecular interference is negligible.[48] Therefore, the following relation holds between ΔR_θ, the weight-average molecular weight of the solute M_w, the second virial coefficient A_2, and c, the weight concentration:[48]

$$Kc/\Delta R_\theta = 1/M_w + 2A_2c \quad (15a)$$

The constant K is given by[49]

$$K = 4\pi^2 n_0^2 (\partial n/\partial c)_{\mu_s}^2/(\lambda_0^4 N_{Av}) \quad (15b)$$

where n_0 is the refractive index of the solvent, $(\partial n/\partial c)_{\mu_s}$ is the increment of the refractive index with concentration measured at constant chemical potential of the solvent (μ_s), and λ_0 and N_{Av} have been defined previously.

Results

Dynamic Light Scattering Experiments. The intensity autocorrelation functions of DNA solutions with concentrations ranging from 0.5 to 18.5 g L^{-1} were measured at angles between 20 and 110°. The results for the apparent diffusion coefficients extracted from the correlation functions by the previously described data analysis methods are summarized in Table I.

Correlation functions of solutions with concentrations lower than ~2 g L^{-1} showed clearly single-exponential behavior. These correlation functions were measured using a single sample time chosen such that the agreement between the measured and calculated base line was within 0.1%. These data were analyzed by the method of cumulants and CONTIN only.

A typical CONTIN output in terms of the frequency distribution function $G(\Gamma)$ is shown in Figure 1. From the moments of $G(\Gamma)$, as given by CONTIN, the average frequency was calculated. The first cumulant agreed very well with the average frequency as computed by CONTIN. The normalized second cumulant was of the order of 0.1, confirming the single-exponential nature of the measured autocorrelation function.

The average frequencies as determined by both methods at various angles were plotted versus the square of the length of the scattering vector q. Results from both analyses showed a linear dependence on q^2 (Figure 2).

Table I
Apparent Diffusion Coefficients (20 °C, 10^{-7} cm^2 s^{-1}) As Determined by the Method of Cumulants, DISCRETE, and CONTIN[a]

			DISCRETE			CONTIN		
c, g L^{-1}	CL^3	CUM: D	D_f	D_s	A_f/A_s	D_f	D_s	A_f/A_s
0.56	1.0	2.2				2.2		1:0
0.73	1.3	2.14				2.14		1:0
1.88	3.4	2.22				2.22		1:0
3.86	7.0	2.40				2.50		1:0
7.43	13.5	2.42	3.47	0.59	2:1	3.13	0.28	2:1
12.5	22.8	3.00	4.01	1.0	3:1	3.43	0.4	6:1
18.6	32.9	3.64	4.3	1.0	17:1	4.04	0.31	10:1

[a] CUM: method of cumulants. c: weight concentration of DNA. D: average apparent diffusion coefficients. D_f, D_s: apparent diffusion coefficients of the fast and slow modes, respectively. A_f/A_s: ratio of the amplitude of the fast mode to the amplitude of the slow mode.

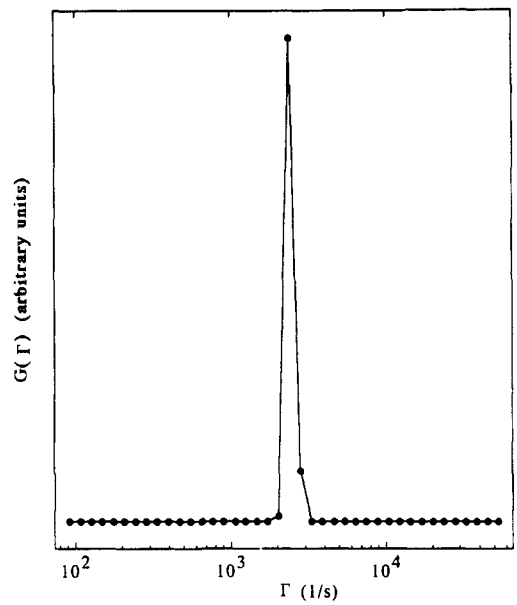

Figure 1. Typical CONTIN output at low DNA concentrations. Depicted is the frequency distribution $G(\Gamma)$ (in arbitrary units) as a function of the frequency Γ (s^{-1}) for a 0.56 (g L^{-1}) DNA solution. The scattering angle was 30°.

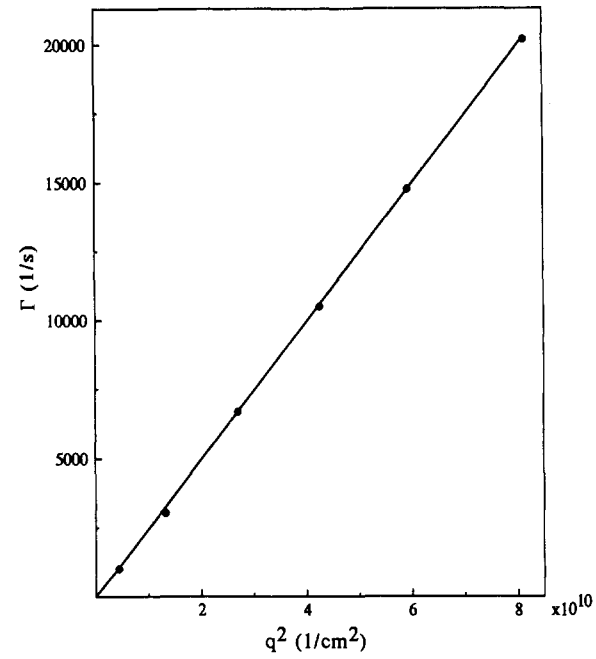

Figure 2. Variation of the average frequency Γ (s^{-1}) as determined by CONTIN with the square of the length of the scattering vector q (cm^{-2}) for a 0.56 (g L^{-1}) DNA solution.

The data were fit to a straight line by the methods of least squares. All fits intersected the ordinate at the origin within the experimental error. The slope of the fits was associated with the apparent diffusion coefficient D_{app}. The results of the cumulant and CONTIN analyses were in excellent agreement (see Table I).

At concentrations between 2 and 7 g/L the experimental correlation function began to deviate from single exponentiality, as was reflected in the larger value of the normalized second cumulant (~0.20). However, it was still possible to sample the correlation function with a single sample time. Data were again analyzed by the method of cumulants and CONTIN.

The results of the CONTIN analysis sometimes gave evidence of two relaxation processes contributing to the autocorrelation function. We refer to the processes with the lower and higher average relaxation frequencies as the slow and fast modes, respectively. Resolution of two modes was very much dependent on the noise in the experimental data. If resolved, the slow mode appeared only at small angles and had an amplitude of less than 4%. Its amplitude decreased with increasing angle. In those instances where CONTIN did resolve two modes, the weighted average of the average frequencies of the two processes was used for further analysis. The first cumulant was usually slightly smaller than the average frequency as determined by CONTIN. When plotted versus q^2, the average frequency as determined by CONTIN and the method of cumulants showed a linear dependence on q^2. From the least-squares linear fit of the data, the apparent diffusion coefficient was determined. The results are tabulated in Table I.

Autocorrelation functions which were measured for solutions with DNA concentrations above 7 g L^{-1} showed pronounced bimodal behavior. It was no longer possible to measure both relaxation times with only one sample time. A set of autocorrelation functions was measured, using a series of sample times. The data were analyzed as before, but in this case data were fit to a sum of two exponentials using DISCRETE.

CONTIN consistently resolved two modes (Figure 3). The average frequency of the fast mode was independent of the sample time used when measuring the correlation function. Variation of the input boundaries of the frequency window of CONTIN had no effect on the results for the fast mode.

In contrast to the results for the fast mode, the results of the CONTIN analysis regarding the slow mode varied considerably with sample time and frequency window. To estimate the average frequency of the slow relaxation process, only correlation functions which showed less than 0.1% difference between the values of the measured and calculated base line were analyzed. The frequency boundaries were set such that both the fast and slow modes were almost fully contained within the frequency window. The results of the CONTIN analysis showed that the amplitude of the slow mode was always much smaller than that of

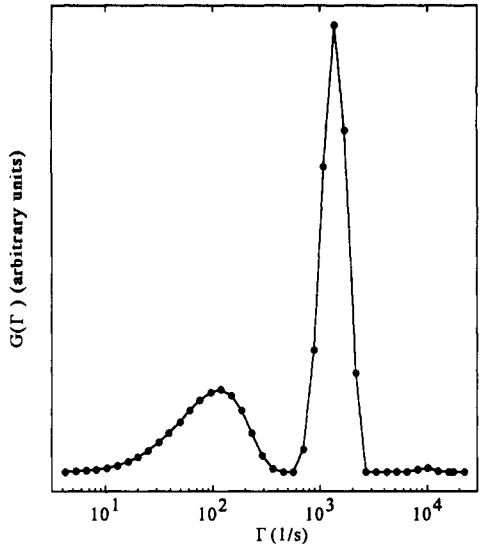

Figure 3. CONTIN frequency distribution $G(\Gamma)$ (in arbitrary units) versus the frequency Γ (s^{-1}) for a 7.4 (g L^{-1}) DNA solution. The scattering angle was 20°.

the fast mode and that it decreased slightly with increasing angle. The frequency distribution of the slow process is much broader than that of the fast mode. In addition, the frequency distribution of the slow mode shows a long "tail" toward the low end of the frequency window. The observed large variation in the results of the CONTIN analysis for the slow mode is probably due to this extremely broad distribution.

The data were also fit to a cumulant expansion up to the second cumulant, although this was strictly speaking no longer applicable because the autocorrelation function deviated largely from single exponentiality in this concentration regime. However, the first cumulant agreed surprisingly well with the weighted average of the average frequencies of the slow and fast mode as determined by CONTIN. As might be expected, the normalized second cumulant was large (>0.3).

The values for the average frequencies of the slow and fast modes, as determined by the double-exponential DISCRETE fit, were consistently higher than those determined by the CONTIN analysis. The results also showed larger variation with sample time. No angular dependence of the amplitude of the slow mode was detected.

The average frequencies at various angles calculated by the three methods of analysis were plotted versus q^2. The frequencies of both the slow and fast mode showed a linear q^2 dependence (Figure 4). The data were fit to a straight line by means of the method of least squares. All fits intersected the origin within experimental error. In general, the data for the fast mode fit a straight line better than those for the slow mode. Data obtained by the CONTIN analysis gave the best fit. Those obtained by the method of cumulants gave the worst fit. From the slope of the fit, D_{app} was determined. The results are given in Table I.

Static Low-Angle Laser Light Scattering Experiments. Data were collected as described, and the Rayleigh ratio ΔR_θ was calculated using eq 14. The value of the constant K was calculated using eq 15b with n_0 = 1.337, $(\partial n/\partial c)_{\mu_s}$ = 0.168 mL/g,[50] and λ_0 = 632.8 nm. $Kc/\Delta R_\theta$ was calculated, and the data were plotted versus the concentration c (Figure 5). A linear relationship was evident, and the data were fit to a straight line by the methods of least squares. From the slope and the intercept of the fit, the second virial coefficient A_2 and the molecular weight M_W, respectively, were determined using eq 15a. We found $A_2 = (7.2 \pm 0.2) \times 10^{-7}$ (mol L g^{-2}) and $M_W = (1.56 \pm 0.05) \times 10^5$ g mol^{-1}. Assuming the average molecular weight of one base pair to be 660, this corresponds to a fragment size of 236 ± 8 bp. It has not escaped our notice that the average molecular weight determined in this study is ~20% larger than reported previously by Fried and Bloomfield[26] for a similar system of sonicated calf thymus DNA. However, these authors used a method of differential fractionation which was different from ours. This may account for the observed discrepancy in the measured molecular weight.

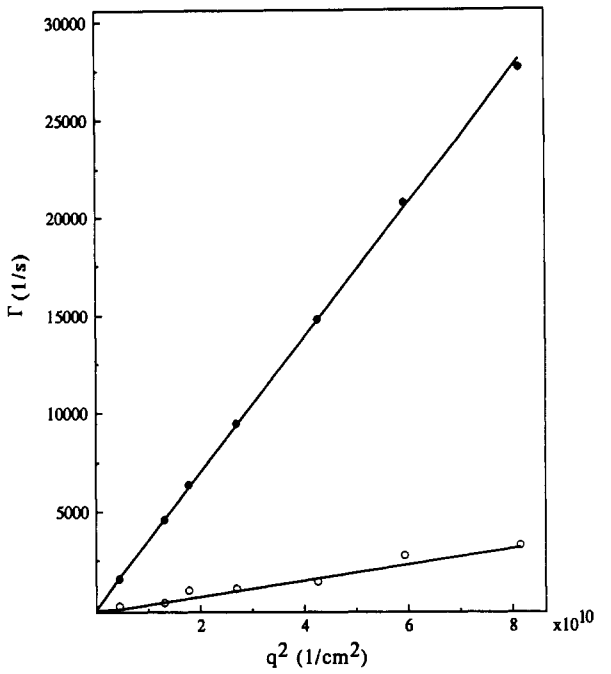

Figure 4. Average frequencies Γ (s^{-1}) of the fast (●) and slow (○) modes for a 18.6 (g L^{-1}) DNA solution determined by CONTIN and plotted versus the square of the length of the scattering vector q (cm^{-2}).

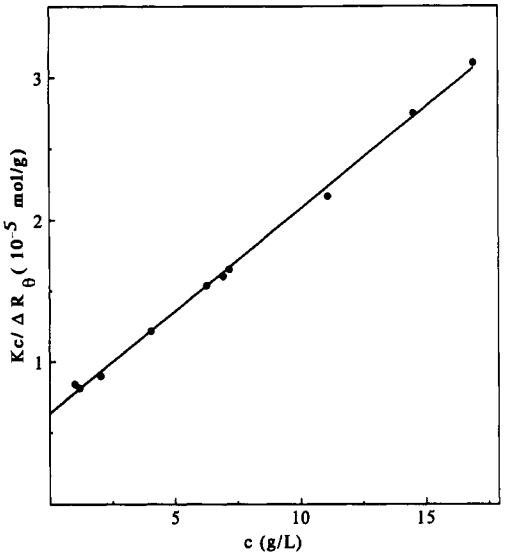

Figure 5. Variation of $Kc/\Delta R_\theta$ (mol/g) with DNA concentration c (g L^{-1}).

Discussion

Data Analysis. The data summary in Table I shows that the apparent diffusion coefficient as determined by the method of cumulants is in good agreement with that calculated by CONTIN for concentrations up to about 2 g

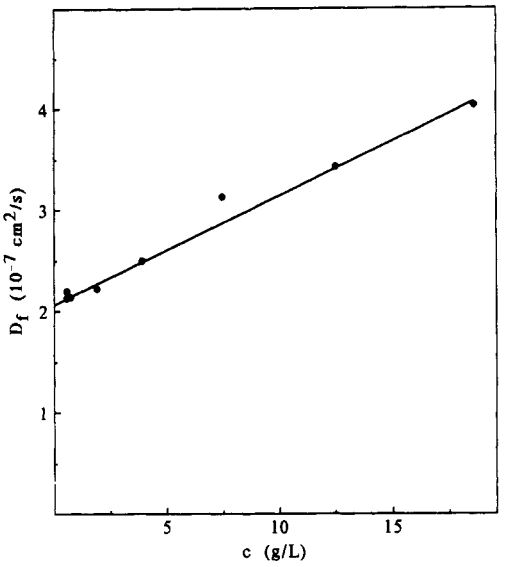

Figure 6. Mutual translational diffusion coefficient of the fast mode D_f (cm^2 s^{-1}) as a function of the DNA concentration c (g L^{-1}).

L^{-1}. At higher concentrations this diffusion coefficient is lower than the D_{app} estimated by CONTIN and DISCRETE. The first cumulant represents the weighted-average frequency over the *whole* frequency domain. Therefore, the observed discrepancy at high concentrations can be ascribed to the presence of the slow mode.

For concentrations above ~7 g L^{-1}, the DISCRETE analysis gives higher values for the average frequencies of the fast and slow modes as compared to the results of the CONTIN analysis. This is probably due to the tendency of DISCRETE to account for more of the long tail of the slow mode in the constant dust factor Q in eq 13. This results in higher values of the apparent diffusion coefficient for both the fast and slow processes (see Table I).

In this study the fast and the slow processes show relatively broad frequency distributions. The polydisperse nature of these processes is best accounted for in the analysis by CONTIN, because a *continuous* rather than a *discrete* frequency distribution is assumed. Also, a major advantage of CONTIN is that no prior knowledge of the number of processes (or peaks in the frequency distribution $G(\Gamma)$) is necessary. In this study the quality of the fit of the average frequency determined by CONTIN versus q^2 was always better than the quality of the fits using the other methods of analysis. The results of the CONTIN analysis varied the least with the sample time which was used to measure the autocorrelation function. Therefore, further discussion of the fast and slow processes will focus on the data given by CONTIN.

Fast Mode. The fast mode was observed over the whole concentration range under study. The fast relaxation process showed up as a relatively narrow peak in the frequency distribution (Figure 1). This indicates that the polydispersity of the DNA fragments is relatively small, which is also confirmed by the small value of the normalized second cumulant at low concentrations. The average frequency of the fast process showed a linear dependence on q^2. The apparent diffusion coefficient of the fast mode was assumed to represent the mutual translation diffusion coefficient D_m. D_m, as determined by the CONTIN analysis, is plotted as a function of concentration in Figure 6.

It is instructive at this point to compare our results to the predictions of the DSO-I theory.[6] The DSO-I theory using the DE assumptions about self-diffusion and rotation predicts systematic fractional deviations $B(C)(qL)^2$ from

Table II
Calculated $B(C)(qL)^2$ as a Function of Concentration at $q^2 = 1.0 \times 10^{11}$ cm^{-2}

c, g L^{-1}	$C/C^* \times 10^3$	dilute × 10^2 (eq 16a)[a]	concd × 10 (eq 16b)[a]
0.56	6.7	0.83	−1.4
0.73	8.7	0.59	−1.5
1.88	22.5	−0.88	−1.6
3.86	46.1	−2.9	−1.8
7.43	88.8	−5.3	−2.0
12.5	149.4	−7.5	−2.3
18.6	222.3	−9.1	−2.4

[a] Using diameter d = 2.6 nm,[53] L = 77.9 nm, and MW = 1.56 × 10^5.

linear behavior in a plot of the initial decay rate versus q^2, where

$$B(C) = \frac{1}{36}\left(\frac{1}{10} - \frac{8C}{(C^* + 8C)}\right) \quad \text{dilute} \qquad (16a)$$

and

$$B(C) = -\frac{1}{9}\left(\frac{1}{5} + \frac{2C}{(C^* + 8C)}\right) \quad \text{semidilute} \qquad (16b)$$

where $C^* = 16/\pi dL^2$. Note that the sign of the deviation is positive at low concentrations and negative at high concentrations. For our system c^* (in weight concentration units) is calculated to be 83.7 g L^{-1}. Table II shows the calculated values of $B(C)(qL)^2$ for our system using the given DNA parameters (see below) at our largest q. Deviations from linear q^2 dependence of the average decay rate using DSO-I and the DE assumptions would be from 1 to 25%. The errors of the average decay rates for the fast mode as determined from CONTIN were on the order of 5%. Thus, the systematic deviations of this type from straight-line behavior for the fast mode should have been observable in plots of the average decay rate versus q^2 at high q and at concentrations from 7.5 to 18.6 g L^{-1}. Using a larger effective diameter for the DNA (see below) would make the discrepancies even larger.

Since the DSO-I theory refers to the initial decay rate, perhaps the average of all the decay times (including the slow mode) as computed from cumulants or the CONTIN moments should instead be used in the comparison with theory. As stated above, the average of all the times for the concentrated samples computed from CONTIN depended on the sampling time and frequency window limits chosen (mainly due to the difficulty of fitting the slow mode) and so was not useful in a comparison. The first cumulant, however, gave a linear q^2 dependence, but this fit was not as good as the separate fits for the average times of the fast and slow modes from CONTIN. In any case, no systematic deviations from linear behavior were observed in the cumulant fits.

This failure of DSO-I could be due to the fact that DSO-I is a theory for hard rods while our system, even though it is at high ionic strength, exhibits Coulomb forces. It is, however, not clear that DSO-I even quantitatively applies to rodlike molecules with no net charge. Russo, Karasz, and Langley (RKL)[11] for instance found systematic deviations from q^2 behavior for the average decay rate (from the first cumulant) of poly(γ-benzyl α,L-glutamate) (PBLG) in dimethylformamide (DMF). Deviations began to be evident at 14.8 g L^{-1} for a system with c^* = 30.0 g L^{-1}. If we compute the $B(C)(qL)^2$ expected from DSO-I for the RKL system, we find that larger deviations are expected than in our case but that the values measured by RKL are considerably smaller in magnitude than predicted.

Table III
Comparison of Experimental with Theoretical Values of D_0 at 20 °C

	$D_0 \times 10^7$, cm^2 s^{-1}
exptl	2.06 ± 0.01
Broersma[a]	1.89
Tirado and Garcia de la Torre[a]	2.06
Yamakawa and Fujii[a]	2.17

[a] Using diameter d = 2.6 nm,[53] persistence length P = 50 nm,[51,60] and rise per base pair RPB = 0.33 nm bp^{-1}.[52]

The mutual translation diffusion coefficient is clearly dependent on the polymer concentration. The critical concentrations as defined by DE for a 236 bp DNA fragment are 0.55 g/L for the $1/L^3$ and 16.4 g/L for the $1/dL^2$ concentration, using d = 2.6 nm and the rise per base pair RPB = 0.33 nm/bp.[51-53] (Small variations in the diameter are not important for rods of this length.[27]) Thus, the highest concentration which was studied (~20 g/L) corresponds to ~35 times the overlap concentration $1/L^3$ given by DE. The highest concentration does not exceed the concentration $1/dL^2$ to a large extent. Thus, the concentration range studied here encompasses the dilute and the semidilute concentration regime as defined by DE. The system may still be considered isotropic.

In the DE theory semidilute behavior for the translational self-diffusion coefficient should be observed at concentrations at least 10 times the overlap concentration $1/L^3$. Figure 6 clearly shows that none of the assumptions of DE for the translational diffusion coefficient in the semidilute concentration regime applies to the mutual diffusion coefficient as measured by our fast mode: the experimental translational diffusion coefficient does not reduce to half its value at infinite dilution, nor is it found to be independent of concentration. These observations are in accordance with the results of previous studies[11,12,14] and the expectation that, since our system is not ideal as shown by the measured nonzero value for A_2, the self-diffusion and mutual diffusion coefficients should not be equal.

Returning to Figure 6, the measured mutual translational diffusion coefficient shows a linear dependence on the concentration in the concentration range studied. Such a linear dependence has also been observed in a similar concentration range for 150 bp mononucleosome DNA.[14] The data were fit to a straight line by the methods of least squares. It was assumed that the theoretical expression for D_m as given by eq 6 is valid for the whole concentration regime under study. D_0 and k_d were determined from the intercept and the slope of the fit, respectively. We found $D_0 = (2.06 \pm 0.01) \times 10^{-7}$ cm^2 s^{-1} and $k_D = 0.052 \pm 0.001$ L g^{-1}.

From the average fragment size of 236 ± 8 bp (determined, as stated above, from the measured average molecular weight), the diffusion coefficient at infinite dilution D_0 can be calculated using the theoretical expressions given by Broersma, Tirado and Garcia de la Torre, and Yamakawa and Fujii. The results of these calculations together with the experimental data are shown in Table III. The calculated value of D_0, calculated according to the Broersma equations, underestimates the value of D_0 slightly. Tirado, Martinez, and Garcia de la Torre[53] compared the theoretical predictions for D_0 by Broersma to experimental results for DNA fragments of various lengths and reported the same observation. The D_0 determined in this study is in excellent agreement with the value given by Tirado and Garcia de la Torre. The value of D_0 for the Yamakawa and Fujii model of a wormlike cylindrical chain is ~5% larger than the experimentally found D_0. Thus, comparison of the experimental and theoretical values for D_0 indicates that DNA fragments with an average size of 236 bp may still be modeled as rigid rods. No flexibility has to be taken into account.

Table IV
Experimental and Theoretical Values of A_2, k_f, and k_D[a]

	$A_2 \times 10^{-7}$, mol L g^{-2}	k_f, L g^{-1}	k_D, L g^{-1}
expt	7.2 ± 0.2	0.08 ± 0.01	0.052 ± 0.001
theory	3.4 ± 0.6	0.2 ● 0.1[c]	
	6.1 ± 0.6[b]		

[a] Unless noted otherwise, the following values were used in the calculation: diameter d = 2.6 nm,[53] solvent viscosity η_s = 1.002 cP, and specific volume $v_s = 0.556 \times 10^{-3}$ L g^{-1}.[54] [b] Using d = 4.41 nm (see text). [c] Error according to Peterson.[41]

We now turn to the discussion of the diffusion virial coefficient k_D. Using eq 6b with $v_s = 0.556 \times 10^{-3}$ L g^{-1},[54] k_f was calculated from the experimentally determined values of k_D, M, and A_2. Theoretical estimates of A_2 and k_f were calculated according to eqs 10 and 11, respectively. The results are summarized in Table IV.

The value of A_2 calculated from the theoretical expression for uncharged rigid rods (eq 10) is much smaller than the experimental value of A_2. Equation 10 was derived assuming *hard-core interactions* only. Electrostatic interactions, even at an ionic strength as high as in this study, might account for the observed disagreement between experiment and theory.

Nicolai and Mandel[13] measured the second virial coefficient in solutions of 150 bp DNA fragments as a function of ionic strength. They found that, due to increased electrostatic interactions, the second virial coefficient increased with decreasing salt concentration. Theoretically, they accounted for the observed charge effects by introducing an effective diameter d_{eff} and an effective length L_{eff} in Ishihara's expression for A_2. L_{eff} and d_{eff} are larger than L and d, respectively. The calculation of these effective parameters is complicated, and the reader is referred to the original paper.

Stigter[55] also calculated an effective diameter dependent on ionic strength. This effective diameter reflects the coil expansion due to electrostatic repulsion. Values of d_{eff} at various salt concentrations are tabulated in his paper. Taking his value of 4.41 nm for the effective diameter of DNA at 0.2 M NaCl and using eq 10, we calculated $A_2 = (6.1 \pm 0.6) \times 10^{-7}$ (mol L g^{-2}) for the solution of 236 bp DNA fragments in our study. This result is in much better agreement with the observed value of A_2 than the value calculated with d = 2.6 nm. These results seem to indicate that, even at salt concentrations as high as 0.2 M NaCl, electrostatic interactions in solutions of polyelectrolytes can have a profound effect on the second virial coefficient.

The theoretical value of k_f as shown in Table IV has been calculated using the expression for k_f given by Peterson[41] (eq 11). It should be stressed that this expression is intended to give only an *estimate* of the real value of k_f. Comparing the theoretical value of k_f to experimental data for the tobacco mosaic virus, Peterson found that the disagreement between these values was ~50%. However, in a study of the dynamics of poly(ε-(carbobenzoxy)-L-lysyl-γ-benzyl L-glutamate) in dimethylformamide (DMF), Itou et al.[56] found that eq 11 predicted the dependence of k_f on the molecular weight rather well. Kubota, Tominaga, and Fujime[57] observed agreement within ~20% between their experimental and theoretical estimates of k_f for a system of PBLG rods in DMF. These studies were done on polymers with molecular weights well above 10^5.

In our study, the theoretical and experimental values of k_f were in poor agreement (see Table IV).

The discrepancy could be due to electrostatic interactions in the solutions of DNA, which were not considered in the derivation by Peterson. Also, some of Peterson's assumptions appear not to be justified for short rods. Clearly, to describe the observed behavior of k_f for (short) rigid rods, more rigorous theoretical calculations are needed. Due to the large error in the theoretical estimate of k_f, no reasonable value for k_D could be calculated from theory.

If we identify the diffusion coefficient corresponding to the fast mode with the D_{coop} discussed by DSO-I,[6] the slope of the D_m vs c plot may be compared to the theoretical predictions. The DSO theory essentially treats the self-diffusion coefficients as parameters. At relatively low concentrations and low q, the DSO-I theory adds nothing new to the predictions of the phenomenological theory (eq 6), except to say that k_f is the same as that for self-diffusion. Since we have not made independent measurements of self-diffusion, this point cannot be further discussed here. However, in the semidilute region in which the self-diffusion coefficient is assumed by DE to be independent of concentration, DSO-I gives $D_m = D_0(1 + 2MA_2c)$. Thus k_D may be easily calculated from the measured A_2 and is found to be 0.226 L g^{-1}, which is more than 4 times the value found experimentally (Table IV). If we use the average apparent diffusion coefficient including the slow mode versus concentration to determine the experimental slope, then the discrepancy would be even larger.

For comparison of our results with those previously reported for different, but similar, systems, it is convenient to introduce the dimensionless parameters K_D, K_t, and K_f. K_D is the linear coefficient in the expansion of the mutual diffusion coefficient in the *volume fraction*, ϕ_v, rather than in c, the *weight concentration*.[5] K_D is related to K_t and K_f by

$$K_D = K_t - K_f \tag{17}$$

where K_t is the virial coefficient which reflects the thermodynamic driving force, while K_f represents the frictional resisting force. The above virial coefficients can be calculated from k_D, A_2, and k_f as

$$K_D = k_D(c/\phi_v) \tag{18a}$$

$$K_t = 2MA_2(c/\phi_v) \tag{18b}$$

$$K_f = (\upsilon_s + k_f)(c/\phi_v) \tag{18c}$$

with the volume fraction ϕ_v given by

$$\phi_v = (N_{Av}V_hc)/M \tag{18d}$$

Here V_h is the volume of one particle in solution, which we have taken to be the volume of a sphere with the measured hydrodynamic radius, R_h. R_h was, as usual, calculated from D_0 using the Stokes–Einstein relation.

Table V shows the values of the virial coefficients calculated from our results and those calculated or obtained from previous work.[13,14,30,31] The quantities K_D, K_t, and K_f are calculated using at least four experimental input parameters, and the estimated errors in the final results are, consequently, relatively large. The data represented in Table IV do, however, show trends as the molecular weight of the DNA is increased.

K_D for large globular DNA molecules is reported to be relatively independent of molecular weight.[30] On the basis of the small amount of data available, this does not seem to hold for the shorter more rodlike DNA fragments. Also, K_D as well as K_t for short DNA fragments appears to be larger than that for long DNA molecules. The relationship between K_D, K_t, and K_f holds very well for the 150 bp DNA fragments at 0.1 M NaCl. However, this was not always the case at all salt concentrations.[14] It should be emphasized that these "volume fraction" expansions and comparisons are based on replacing the single particle volume V_h by the volume of a sphere with radius R_h. The volume used, thus, is closer to the actual molecular volume for the larger more globular DNAs than it is for the shorter more rodlike ones.

Table V
Diffusion and Virial Coefficients of Linear DNA Molecules

L, bp	$M_w \times 10^5$	$D_0 \times 10^7$, cm^2 s^{-1}	K_D	K_t	K_f
152[a]	1.00 ± 0.02	3.04 ± 0.05	10 ± 1	13 ± 4	3 ± 1
236	1.56 ± 0.05	2.06 ± 0.01	2.9 ± 0.2	12 ± 1	9 ± 1[d]
2311[b]	15.3	0.442	1.3 ± 0.3		
6515[c]	43.0	0.198	1.12 ± 0.03	6.23	2.57 ± 0.72

[a] Calculated from the results reported by Nicolai and Mandel[13,14] for mononucleosome DNA at 0.1 M NaCl. [b] From Sorlie and Pecora[30] for linearized pLH2311 plasmid DNA at 0.1 M NaCl. [c] Calculated from the data reported by Voordouw et al.[31] for linearized ColE1plasmid DNA at 0.2 M NaCl. [d] Calculated from the K_D and K_t according to $K_D = K_t - K_f$.

Slow Mode. A relaxation process with a relatively large decay time has been reported for systems of various polylectrolytes.[11-21] In solutions of short rodlike polyelectrolytes, the slow mode has been observed at low ionic strength and high polyion concentration. The polymer concentration at which the slow mode began to appear decreased with decreasing ionic strength.[14] Drifford and Dalbiez[19] described the same observation for aqueous solutions of high molar mass sodium poly(styrene sulfonate), where the slow mode appeared at a fixed ratio of polyion concentration to salt concentration. In our study, CONTIN gave evidence of an additional slow process at concentrations as low as 2 g/L. However, due to the small amplitude of the slow mode at lower concentrations, consistent results for the slow mode could only be obtained for concentrations higher than about 7 g L^{-1}.

Generally, for high molecular weight polyelectrolytes a relatively sudden transition is observed from a region were the fast mode is preponderant to a region where the slow mode dominates.[18-21] However, we found that the two modes coexist over a rather broad polymer concentration range (about 2–20 g/L). This is in accordance with the results of previous studies on similar systems of low molar mass DNA.[14] We comment on this observation below.

The frequency of the slow relaxation process was typically 1 order of magnitude smaller than the relaxation frequency of the fast process. The average frequency of the slow mode showed a linear dependence on the square of the length of the scattering vector q. The amplitude of the slow mode decreased slightly with increasing angle. From the above results, it may be concluded that the slow mode reflects a diffusion process, which is caused by fluctuations which take place on a length scale which is large relative to the probing distance $1/q$. The apparent diffusion coefficient corresponding to this mode is given in Table I. These observations on the slow relaxation frequency are in agreement with the results previously reported for systems of short rodlike polyelectrolytes as well as for systems of long flexible polyelectrolytes.

The origin of the slow mode has been the subject of extensive study and discussion but is still speculative. Several explanations have been brought forward. Schmitz

Table VI
Ratios of Amplitudes and Apparent Diffusion Coefficients of the Fast and Slow Modes

		DSO-II theory[a]		exptl	
c, g L^{-1}	$C/C^* \times 10^3$	A_f/A_s	D_f/D_s	A_f/A_s	D_f/D_s
0.56	6.7	0.58	6.31		
0.73	8.7	0.59	6.28		
1.88	22.5	0.69	6.13		
3.86	46.1	0.88	6.00		
7.43	88.8	1.28	6.05	2.0	11.2
12.5	149.4	1.99	6.51	6.0	8.6
18.6	222.3	3.08	7.50	10.0	13.0

[a] Calculated from eqs 2.23, 4.8, 4.11, and 4.12 of Doi, Shimada, and Okano.[8]

and Lu[15] considered coupling of the translational and rotational modes to be responsible for the slow mode. As was pointed out by Bloomfield,[58] this possibility can be ruled out for short rigid rods. It has been shown that the dynamic light scattering of solutions of polydisperse, strongly interacting polymers can, under certain conditions, measure the *self*-diffusion coefficient in addition to the *mutual* diffusion coefficient.[32] Let us assume that these conditions apply to a system of short DNA fragments. For a system of 150 bp nucleosome DNA, the self-diffusion coefficient was measured independently using forced Rayleigh light scattering techniques.[12] It was found that the self-diffusion coefficient did not coincide with the diffusion coefficient of the slow mode D_s and did not show the same dependence on ionic strength. These results imply that the diffusion coefficient of the slow mode is not the same as the self-diffusion coefficient of unaggregated DNA. Fried and Bloomfield[26] suggested the existence of a gellike phase in semidilute solutions of 200 bp DNA fragments. According to these authors, the gellike phase gives rise to a slow mode in the autocorrelation function of the scattering intensity. However, they reported that the gellike phase was *stabilized* by small ions. The slow mode on the contrary is found to be more prominent at *low* ionic strength.

An alternative explanation of the slow mode may be sought in the DSO spinodal decomposition theory.[8] This theory is constructed for solutions near the critical composition $C^* = 16/\pi dL^2$ at which the isotropic phase becomes unstable. If the concentration of the solution is suddenly brought above C^*, an anisotropic phase separates from the isotropic phase by spinodal decomposition. For solutions in the isotropic phase near C^*, DSO-II predicts that the dynamic structure factor at small q should consist of two exponentials whose amplitude and relaxation time ratios depend on C and C^* (eqs 2.23, 4.8, 4.11 and 4.12 of ref 8). For our system of sonication fragments, using the diameter of 2.6 nm, we find that at the highest concentration in our study C is only $0.2C^*$. We have, nonetheless, compared our values for the amplitude and relaxation time ratios with the predictions of DSO-II.[8] The results are shown in Table VI. There is poor agreement between DSO-II and our experimental results. Use of the Stigter larger effective diameter discussed above does not result in any improvement.

At the present, the most plausible explanation of the slow mode seems to be the formation of aggregates at high concentrations. The aggregates are assumed to be large relative to $1/q$. Aggregation is to be favored by low concentrations of low molar weight salt. The formation of aggregates is supported by previous observations that the slow mode disappears after filtration through 0.22- and 0.05-μm pore size filters.[12-14] The slow mode was first detectable again ~5 min after filtration. Equilibrium was reached ~30 min thereafter. In our LALLS experiments, we observed an increased fluctuation of the scattering intensity after filtration through 0.45-μm pore size filters instead of 0.22-μm pore size filters. The average size of the aggregates is apparently smaller than 0.45 μm.

Yet, the concept of aggregation is hard to reconcile with the results of the forced Rayleigh experiments on 150 bp nucleosome DNA.[12] These experiments gave no indication of any significant change of the behavior of the self-diffusion coefficient at low ionic strength. Schmitz et al.[25] proposed an explanation for a similar inconsistency observed for saline solutions of poly(L-lysine). They considered the effects of small ions on the dynamics of the polyion. It was suggested that the slow mode represents the *dissolution* of so-called "temporal" aggregates rather than the *translational diffusion* of these large structures. With this assumption, these authors argued that the "average" environment of a single poly(lysine) particle was not expected to change drastically with ionic strength, which would explain the relatively constant behavior of the experimental self-diffusion coefficient. More study is necessary to confirm this hypothesis. Apart from the described discrepancy, the formation of aggregates is consistent with all the data regarding the slow mode presently available.

As to the mechanism of aggregation, Bloomfield[58] suggested the formation of colloidal crystals, which are stabilized solely by repulsive electrostatic force.[32] Such has been observed recently by Pedley et al. in solutions of sulfonated polystyrene in xylene.[59] As proposed by Schmitz et al.,[25] the aggregates might arise as the result of a balance between attractive dipole forces, which are due to the sharing of small ions by several polyions, and repulsive electrostatic and Brownian diffusion forces. The coupling between the small ions and the polyions would be impaired at high ionic strength due to screening effects.

The results presented here are consistent with the formation of aggregates at high polymer concentrations. The rather broad frequency distribution of the slow process is probably due to the highly polydisperse nature of the aggregates. The small amount of data presented do not justify any definite conclusions but may help clarify the characteristics of the slow mode.

The diffusion coefficient as well as the amplitude of the slow mode seems to decrease with increasing concentration after an initial increase when the slow mode first appears (see Table I). The decrease of the slow relaxation frequency with increasing concentration may be due to an increase in the average size of the aggregates. Mathiez et al. observed the same trends for the frequency and amplitude of the slow mode in saline solutions of high molecular weight poly(adenylic acid).[20,21] It was suggested that the slow mode may only be observed in the range of intermediate concentrations. At low concentrations, the amplitude is too small to be determined and, for higher concentrations, the frequency of the slow mode is too small to be distinguished from the background of static scatterers. This may explain the rather narrow concentration range over which the slow and fast modes coexist in systems of high molar mass polyelectrolytes, as compared to the rather broad coexistence range observed in systems of low molar mass DNA.

Conclusion

DLS studies of the dynamics of 236 bp DNA fragments at high ionic strength (0.2 M NaCl) follow rigid-rod behavior in dilute solution. In semidilute solutions the DLS intensity autocorrelation functions began to deviate from single exponentiality at a DNA concentration of about

2 g/L. CONTIN, which appears to be more capable than cumulants and two-exponential DISCRETE fits in analyzing complex autocorrelation functions, consistently gave two modes at concentrations above 7 g/L, one of which, the slow mode, has a rather broad frequency distribution.

The fast mode reflects the translational diffusion of the DNA molecules. The mutual diffusion coefficient extracted from the fast-mode decay frequency was observed to increase linearly with the DNA concentration. The experimental value of the translational diffusion coefficient at infinite dilution is in excellent agreement with the theoretical predictions for rigid rods of Tirado and Garcia de la Torre, indicating that DNA fragments with a fragment size of 236 bp may still be modeled as rigid rods. The experimental value of the thermodynamic virial coefficient, A_2, is in poor agreement with the theoretical value calculated using a diameter of 2.6 nm. Agreement is better if an enlarged effective diameter, calculated according to Stigter's theory, is used in the calculation, indicating that even at 0.2 M NaCl charge effects cannot be neglected entirely. Peterson's theoretical expression for the friction second virial coefficient, k_f, did not predict the experimental value very well. More rigorous theoretical work on this quantity for rigid rods should be undertaken. Longer DNAs which exhibit more flexibility show very different second virial coefficients from the short sonication fragments.

The present results for the slow mode are consistent with the formation of large aggregates at high DNA concentrations. Theories of DLS from hard rigid rods such as DSO-I[6] and the spinodal decomposition theory given in DSO-II[8] are in poor agreement with our experimental results. The presumed aggregates are probably highly polydisperse. There is circumstantial evidence that the aggregates increase in size as the polymer concentration is increased.

Acknowledgment. This work was supported by National Science Foundation Grant CHE-88-14641 to R.P. and by the NSF–MRL program through the Center for Materials Research at Stanford University. Dr. Joachim Seils, Adam Cantor, John Tracy, and Mark Tracy gave invaluable assistance during the course of this work. H.T.G. is greatly indebted to DSM Limburg B.V. for their financial support of his stay at Stanford University.

References and Notes

(1) Doi, M. *J. Phys. (Paris)* **1975**, *36*, 607. Doi, M.; Edwards, S. F. *J. Chem. Soc., Faraday Trans. 2* **1978**, *74*, 560.
(2) Doi, M.; Edwards, S. F. *The Theory of Polymer Dynamics*; Clarendon Press: Oxford, 1986.
(3) Fixman, M. *Phys. Rev. Lett.* **1985**, *54*, 337; **1985**, *55*, 2429.
(4) Bitsanis, I.; Davis, H. T.; Tirrell, M. *Macromolecules* **1988**, *21*, 2824; **1990**, *23*, 1157.
(5) Berne, B. J.; Pecora, R. *Dynamic Light Scattering*; Krieger Publishing Co.: Malabar, FL, 1990.
(6) Doi, M.; Shimada, T.; Okano, K. *J. Chem. Phys.* **1988**, *88*, 4070.
(7) Maeda, T. *Macromolecules* **1989**, *22*, 1881; **1990**, *23*, 1464.
(8) Doi, M.; Shimada, T.; Okano, K. *J. Chem. Phys.* **1988**, *88*, 7181.
(9) Maier, K. R. Ph.D. Thesis, Stanford University, Stanford, CA, 1986.
(10) Zero, K. M.; Pecora, R. *Macromolecules* **1982**, *15*, 87.
(11) Russo, P. S.; Karasz, F. E.; Langley, K. H. *J. Chem. Phys.* **1984**, *80*, 5312.
(12) Wang, L.; Garner, M. M.; Yu, H. *Macromolecules* **1991**, *24*, 2368.
(13) Nicolai, T.; Mandel, M. *Macromolecules* **1989**, *22*, 438.
(14) Nicolai, T.; Mandel, M. *Macromolecules* **1989**, *22*, 2348.
(15) Schmitz, K. S.; Lu, M. *Biopolymers* **1984**, *22*, 797.
(16) Fulmer, A. W.; Benbasat, J. A.; Bloomfield, V. A. *Biopolymers* **1981**, *20*, 1147.
(17) Lin, S.; Lee, W.; Schurr, J. M. *Biopolymers* **1978**, *17*, 1041.
(18) Zero, K.; Ware, B. R. *J. Chem. Phys.* **1984**, *80*, 1610.
(19) Drifford, M.; Dalbiez, J. *Biopolymers* **1985**, *24*, 1501.
(20) Mathiez, P.; Weisbuch, G.; Mouttet, C. *Biopolymers* **1979**, *18*, 1465.
(21) Mathiez, P.; Mouttet, C.; Weisbuch, G. *Biopolymers* **1981**, *20*, 2381.
(22) Kubota, K.; Chu, B. *Macromolecules* **1983**, *16*, 105.
(23) Keep, G.; Pecora, R. *Macromolecules* **1988**, *21*, 817.
(24) Aragon, S. R.; Pecora, R. *J. Chem. Phys.* **1985**, *82*, 5346.
(25) Schmitz, K. S.; Lu, M.; Singh, N.; Ramsay, D. J. *Biopolymers* **1984**, *23*, 1637.
(26) Fried, M. G.; Bloomfield, V. A. *Biopolymers* **1984**, *23*, 2141.
(27) Pecora, R. *Science* **1991**, *251*, 893.
(28) Mandel, M. *Encyclopedia of Polymer Science and Engineering*; Wiley: New York, 1988; Vol. 11, pp 739–829.
(29) Sorlie, S.; Pecora, R. *Macromolecules* **1990**, *23*, 487.
(30) Sorlie, S.; Pecora, R. *Macromolecules* **1988**, *21*, 1437.
(31) Voordouw, G.; Kam, Z.; Borochov, N.; Eisenberg, H. *Biophys. Chem.* **1978**, *8*, 171.
(32) Pusey, P. N.; Tough, R. J. A. In *Dynamic Light Scattering: Applications of Photon Correlation Spectroscopy*; Pecora, R., Ed.; Plenum Press: New York, 1985.
(33) Schmitz, K. S. *Dynamic Light Scattering by Macromolecules*; Academic Press: San Diego, CA, 1990.
(34) Broersma, S. *J. Chem. Phys.* **1960**, *32*, 1632; **1981**, *74*, 6989.
(35) Tirado, M. M.; Garcia de la Torre, J. *J. Chem. Phys.* **1979**, *71*, 2581.
(36) Yamakawa, H.; Fujii, M. *Macromolecules* **1973**, *6*, 407.
(37) Zimm, B. H. *J. Chem. Phys.* **1946**, *14*, 164.
(38) Onsager, L. *Ann. N.Y. Acad. Sci.* **1949**, *51*, 627.
(39) Ishihara, A. *J. Chem. Phys.* **1950**, *18*, 1446; **1951**, *19*, 1142.
(40) Ishihara, A.; Hayashida, T. *J. Phys. Soc. Jpn.* **1951**, *6*, 40, 46.
(41) Peterson, J. M. *J. Chem. Phys.* **1964**, *40*, 2680.
(42) Kirkwood, J. G.; Riseman, J. *J. Chem. Phys.* **1956**, *8*, 512.
(43) Lis, J. T.; Schleif, R. *Nucleic Acids Res.* **1975**, *2*, 383.
(44) Stock, R. S.; Ray, W. H. *J. Polym. Sci., Polym. Phys. Ed.* **1985**, *23*, 1393.
(45) Koppel, D. E. *J. Chem. Phys.* **1972**, *57*, 4814.
(46) Provencher, S. W. *Comput. Phys. Commun.* **1982**, *27*, 213, 229.
(47) Provencher, S. W. CONTIN's User Manual. Technical Report ENBL-DA02; European Molecular Biology Laboratory: Heidelberg, 1980.
(48) Kratochvil, P. In *Light Scattering from Polymer Solutions*; Huglin, M. B., Ed.; Academic Press: New York, 1982.
(49) For vertically polarized incident and detected light, K is usually half of the value given here. However, in the Chromatix KMX-6 the intensity of the scattered light is measured with an *annulus*. Integration over the segment of the solid angle covered by the annulus leads to multiplication of K by a factor of 2 (at small angles).
(50) Jolly, D.; Eisenberg, H. *Biopolymers* **1976**, *15*, 61.
(51) Elias, J. G.; Eden, D. *Macromolecules* **1981**, *14*, 410.
(52) Elias, J. G.; Eden, D. *Biopolymers* **1981**, *20*, 2369.
(53) Tirado, M. M.; Martinez, C. L.; Garcia de la Torre, J. G. *J. Chem. Phys.* **1984**, *81*, 2047.
(54) Gray, H. B.; Hearst, J. E. *J. Mol. Biol.* **1968**, *35*, 111.
(55) Stigter, D. *Macromolecules* **1985**, *18*, 1619.
(56) Itou, S.; Nishioka, N.; Norisuye, T.; Teramoto, A. *Macromolecules* **1981**, *14*, 904.
(57) Kubota, K.; Tominaga, Y.; Fujime, S. *Macromolecules* **1986**, *19*, 1604.
(58) Bloomfield, V. A. In *Reversible Polymeric Gels and Related Systems*; Russo, P. S., Ed.; American Chemical Society: Washington, DC, 1987.
(59) Pedley, A. M.; Higgins, J. S.; Pfeiffer, D. G.; Rennie, A. R. *Macromolecules* **1990**, *23*, 2494.
(60) Manning, G. S. *Biopolymers* **1981**, *20*, 1751.